THE JOURNAL OF PHYSICAL CHEMISTRY C

Article

pubs.acs.org/JPCC

Experimental and vdW-DFT Study of the Structure, Properties, and Stability of Isonicotinic Acid Self-Assembled Monolayers on Gold

María L. Para,[†] Omar E. Linarez Pérez,[†] Mariana I. Rojas,*[,‡] and Manuel López Teijelo*[,†]

[†]INFIQC, Departamento de Fisicoquímica, Facultad de Ciencias Químicas, and [‡]INFIQC, Departamento de Matemática y Física, Facultad de Ciencias Químicas, Universidad Nacional de Córdoba, H. de la Torre y M. Allende, C. Universitaria, 5000 Córdoba, Argentina

ABSTRACT: Self-assembling of derivatized aromatic molecules on metals is of interest in the generation of modified surfaces with ionizable groups in order to generate charged surfaces for constructing more complex nanostructured interfaces. In the present contribution we explore the structure, properties, and stability of isonicotinic acid (INA) adsorbed on gold surfaces employing electrochemical and spectroscopic methods as well as DFT calculations at the level of van der Waals interactions (vdW-DFT). Electrochemical results show changes in the kinetics of redox probes due to the self-assembled monolayers (SAMS) formation on the gold surface. Furthermore, SERS experiments indicate that INA species adsorb on gold perpendicularly to the surface through the deprotonated carboxylate group. In addition, due to the ionizable groups involved in the molecular anchorage, some instability of the SAMS of INA is obtained by pH modification of the chemical environment. On the other hand, theoretical calculations indicate that a strong interaction of the carboxylate group to the gold surface at the bridge sites takes place, and the adsorbed species have sufficient mobility at room temperature. The effect of the coverage and the stability of the SAMS are also reported.

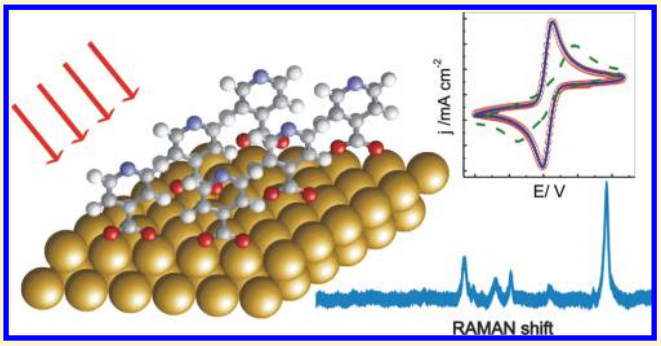

INTRODUCTION

The study of monocrystalline metal surfaces modified by self-assembled monolayers (SAMS) of (bio)molecules is of technological importance due to its application in the development of biomedical devices and biosensors of high selectivity.[1−4] Additionally, molecular self-assembling is a key concept in supramolecular chemistry and nanoscience since it allows the construction of complex molecular architectures though electrostatic interactions. In general, molecules employed in the construction of SAMS are organic molecules composed of an anchorage group that links the molecules to the surface, a spacer group that may be an aliphatic chain or an aromatic ring, and a terminal group in contact with the environment (e.g., an electrolyte), which confers new properties to the surface. The study of self-assembly mechanisms allows understanding the interactions that determine the morphology of the monolayers during nanofabrication processes.[5−7]

During surface modification, molecule−substrate interactions, diffusion of the molecules on the surface or mediated by the solution (as in the case of modification by dipping), nucleation and growth processes, and aggregation of islands (ripening) can take place.[7] In the case of aromatic molecules, $\pi-\pi$ attractive interactions between neighbor molecules appear, favoring formation of domains with an ordered packing, which are commensurate to and with the same symmetry of the surface. Since the layers are often discontinuous, it is important to know the distribution of the exposed areas that remain unchanged.[5] Then, the uncovered areas may present electroactive response and can be easily evaluated by electrochemical techniques.[8−10]

It has been shown that adsorption of organothiols and derivatives confers interesting properties to metallic substrates because of the strong thiolate chemical bonds formed, where the intermolecular interactions of the additional chemical groups may contribute modifying the packing in the SAMS.[8,11−15] In addition, if the adsorbed molecules present ionizable groups exposed to the environment, they offer the possibility of constructing more complex nanostructured interfaces that are sensitive to pH changes. In spite of the wide use of derivatized thiols, isonicotinic acid (INA) has interesting chemical properties, presenting a carboxylic acid group, a nitrogen atom in the pyridine ring, and the π system in the pyridine ring itself. Then, once a monolayer has been formed on the substrate and according to the molecular orientation, ionization of INA groups by modifying the pH of the medium may take place exposing a net charge to the solution. This would allow the construction of more complex nanostructured interfaces as those resulting from the layer-by-layer method.[16] In addition, removal of the surface modification can be also a simple process by means of a pH change, which allows recovering the metallic surface without damage.

Received: November 13, 2015
Revised: February 2, 2016
Published: February 17, 2016

DOI: 10.1021/acs.jpcc.5b11146
J. Phys. Chem. C 2016, 120, 4364−4372

Modified surfaces with a periodic arrangement of charge are of technological importance in the manufacture of nanostructured platforms with pharmacological applications.[17] On the other hand, the effect of the INA molecule backbone on the electron transfer with redox species in solution across self-assembled monolayers or in more complex nanostructures is also of primary interest.[18,19]

Recently, Xu et al.[6] studied by scanning tunnel microscopy (STM) the structure of SAMS of INA adsorbed on Ag (111) deposited by evaporation at ultrahigh vacuum (UHV) conditions. They showed that the acid group remains protonated, and the molecules are assembled parallel to the silver surface. Also, they explained the observed configuration by taking into account the formation of hydrogen bonds between the carboxylic groups and the nitrogen atoms of the pyridine ring in neighbor INA molecules in order to stabilize the layer.[6] On the contrary, Raman spectroscopic studies of nicotinic acid isomers on Ag surfaces[20,21] or colloidal nanoparticles of silver[13] modified by immersion in aqueous solutions indicate that INA is adsorbed onto the Ag surface as an anionic species and the main interaction is through the carboxylate group. In addition, depending on the electrochemical potential applied, the INA molecules may adsorb perpendicular or parallel to the surface due to the $\pi-\pi$ ring interaction between the molecules or π interaction with the Ag surface, respectively.[20]

The aim of this work is to understand the mechanisms involved in the generation of ionizable surfaces by chemical modification in order to generate charged surfaces for constructing nanostructured platforms. Specifically, we study the adsorption and self-assembly of isonicotinic acid on Au (111) surfaces. In the first part, we present the electrochemical and the spectroscopic evidence of the absorption process. In the second part, we study the chemical interactions involved in the adsorption process and the stability of the INA molecular layers adsorbed on Au surface by means of density functional theory (DFT) calculations taking into account van der Waals interactions.[23−26]

We show that a strong interaction of the carboxylate group to the gold surface takes place, thus providing an unexplored novel platform for nanoscience applications (e.g., in the field biosensors) as opposite to the traditional use of alkanethiols or derivatives on gold. This would serve as a robust linking with other nanostructured materials for developing new composite materials.

EXPERIMENTAL AND CALCULATION DETAILS

Apparatus and Electrodes. A conventional three-electrode electrolysis cell with a reference saturated calomel electrode (SCE) and a Pt auxiliary electrode was employed. All potentials were referred to the SCE potential. Working electrodes were deposits of Au on glass slides of 11 × 11 mm^2 purchased from Arrandee or polycrystalline gold rods (Alfa Aesar, 99.9985% purity). The electrolyte was deaerated by bubbling with nitrogen prior to each experiment.

Cyclic voltammetry measurements were carried out at room temperature with an Autolab PGSTAT100 electrochemical interface using the NOVA 1.8 software package.

Surface enhanced Raman spectroscopy (SERS) experiments were performed *ex situ* (in air) using a Horiba LabRAM HR spectrometer, employing a He/Ne laser (632.8 nm wavelength). For the analysis of the spectra, the vibrational modes were represented using the common nomenclature: δ: bending; ν: stretching; τ: torsion; the subscript *as* indicated an asymmetric mode.[23,27,28] The nomenclature proposed by Wilson[27] and Lord[28] was also indicated in parentheses.

Preparation of the Substrates. For the electrochemical measurements, the Au surfaces were electrochemically cleaned by 10 min cycling at 1 V s^{-1} between −1.2 and 0.7 V in a 0.1 M NaOH solution. After that the electrode was immersed in "piranha" solution (3:1 mixture of concentrated sulfuric acid and 30% hydrogen peroxide solution) for 1 min and rinsed with deionized water. In order to promote the development of the Au(111) surface, cleaned electrodes were annealed in a butane flame during 2 min, cooled under constant N_2 flux, and placed immediately in contact with the dipping solution. In order to perform SERS measurements, a polycrystalline gold rod was electrochemically roughened by applying a potential step at +2.4 V for 10 min in a 0.5 M H_2SO_4 solution. Then, a linear potential sweep at 0.02 V s^{-1} from +2.4 to −0.6 V was applied.[29] Finally, the roughened gold surface generated after this procedure was rinsed with deionized water and immersed in the dipping solution.

Preparation of SAMS. All chemicals, isonicotinic acid (4-pyridinecarboxylic acid; Alfa Aesar, 98+% purity), sulfuric acid (Anedra), and sodium hydroxide (Baker) were used as received without further purification. Self-assembled monolayers were prepared by immersing the gold substrates in 10 mM INA + 0.1 M NaOH (pH 13) or 10 mM INA + 1 M H_2SO_4 (pH 0.3) solutions for different dipping times. After the surface modification, the samples were removed from the dipping solution, rinsed with 0.1 M NaOH or 1 M H_2SO_4 solutions, and transferred to the electrolytic solution.

Reagents and Solutions. For electrochemical characterization, 1 M H_2SO_4 deaerated solutions were employed as electrolyte. 5 mM Fe^{2+}/Fe^{3+} (Baker) + 1 M H_2SO_4 (Anedra) solutions were employed as redox probes. For SERS measurements, SAMS of INA prepared on the roughened gold substrates were immersed for 36 h in 10 mM INA + 1 M H_2SO_4 or 10 mM INA + 0.1 M NaOH (pH 0.3 or 13, respectively) solutions and then were rinsed with 1 M H_2SO_4 or 0.1 M NaOH solutions before the experiments.

Theoretical Modeling and Computations. Energy calculations were performed at the density functional theory (DFT) level using the SIESTA code.[23] Core electrons were replaced by norm conserving pseudopotentials, built with the Troullier−Martins recipe[30,31] to represent the nucleus and the core electrons of the considered species. In the pseudopotentials description of the atoms, only electronic valence states were considered. The basis set used for expanding in eigenstates was composed of double-ζ-polarized numerical atomic orbitals (NAOs), which were solutions of the Kohn−Sham Hamiltonian for isolated pseudoatoms. Exchange and correlation effects were described in the generalized gradient approximation (GGA) with Perdew−Burke−Ernzerhof (PBE) functional.[32] The energy of confinement (Energy-Shift) was 50 meV, which was an optimum value to obtain the best accuracy and computational efficiency for this system. The energy cutoff (Mesh-Cut-Off) used was 150 Ry.

The minimum-energy configuration was determined by the conjugate gradient technique,[33] which minimizes the system energy from an initial configuration with respect to the atomic coordinates until the force on each atom was less than 0.04 eV/Å. The minimum-energy path (MEP) was optimized by means of the nudged elastic band method (NEB).[34,35]

DOI: 10.1021/acs.jpcc.5b11146
J. Phys. Chem. C 2016, 120, 4364−4372

All the calculations were performed with spin polarization (sp). van der Waals interactions were taken into account, and the C_6 coefficients in eV Å^6 used were: Au: 220, H: 2.21, C: 15.19, O: 6.08, and N: 10.68, and the van der Waals radii in Å were: Au: 1.48, H: 1.00, C: 1.46, O: 1.34, and N: 1.45.[24−26]

The atomic charges were evaluated by means of the Mulliken population analysis.[36] The Au(111) surface was modeled as a four-layer gold slab with ABC stacking within a tetrahedral unit cell with periodic boundary condition at x, y, z. The optimized lattice parameter for the bulk fcc gold substrate was a = 4.19 Å.

RESULTS AND DISCUSSION

Experimental Evidence. Isonicotinic acid molecule has three chemical groups that can interact with a metallic substrate: the carboxylic acid group, the nitrogen atom in the pyridine ring, and the π system in the pyridine ring itself. In aqueous solutions, depending on pH, different INA species can exist according to the chemical equilibriums shown in Scheme 1.[37] Once a monolayer has been formed and according to the adsorbate orientation, ionization of INA groups by modifying the pH of the medium may take place exposing a net charge to the solution. This is a useful property of the modified surface in order to build nanostructured platforms by electrostatic interactions.

Scheme 1. Acid−Base Equilibriums of INA in Aqueous Solutions

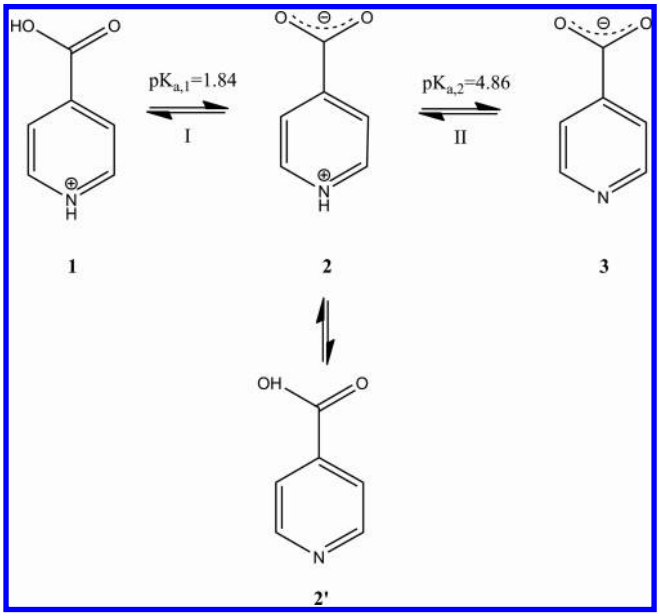

Well-behaved redox couples are usually employed in order to make evident surface modifications as well as to evaluate the blocking properties of monolayer-coated electrodes. They can also provide structural information on the layers, i.e., geometrical coverage.[38,39]

Figure 1 shows the j/E potentiodynamic response at 0.05 V s^{-1} of bare and modified Au (111) electrodes in a 10 mM Fe^{2+}/Fe^{3+} (pH 0.3) solution for different dipping conditions. On the bare gold surface, the Fe^{2+}/Fe^{3+} redox couple shows a quasi-reversible j/E response, with ca. 80 mV of anodic to cathodic peak potentials separation, ΔE_p, and the typical shape for a charge transfer process controlled by semi-infinite linear diffusion.[40] On the other hand, the j/E potentiodynamic response of modified Au surfaces by 36 h of dipping in 10 mM

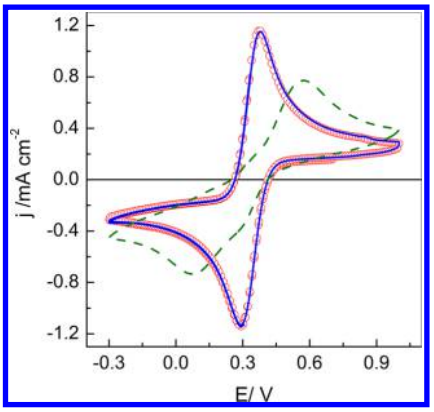

Figure 1. Potentiodynamic j/E response at 0.05 V s^{-1} in a 10 mM Fe^{2+}/Fe^{3+} + 1 M H_2SO_4 solution (pH 0.3) for bare (○) and modified Au(111) electrodes for different pH dipping solutions for 36 h: (- - -) 10 mM INA, pH 0.3, and (—) 10 mM INA, pH 13.

INA (pH 0.3) shows a pronounced increase of ΔE_p reaching ca. 500 mV and a decrease of the peak current for both the anodic and the cathodic current peaks. The small current contributions at the normal potential of the redox couple are attributed to macroscopic uncovered zones at the surface.

This behavior indicates an apparent inhibition of the redox couple kinetics due to the presence of INA adsorbed onto the gold surface, which can be interpreted as a microelectrode array formation[39] where defects and pinholes allow radial diffusion of ionic species of the redox probe, opposite to the behavior on bare gold surfaces where only semi-infinite diffusion takes place. Contrarily, when the dipping is made in alkaline INA solutions (pH 13), the absence of changes in the j/E response for the Fe^{2+}/Fe^{3+} redox probe in acidic media compared to that obtained for the bare gold surface would indicate that the INA molecules have been desorbed in the measurement acidic solution due to the increase in proton concentration. According to these findings, the adsorption of INA molecules onto the Au surface may involve the interaction of any of the ionizable groups (carboxylic acid and/or N in pyridinic ring) with the gold surface.

SERS is a widely used technique for investigating adsorbate−metal interactions in molecular assemblies.[8,9,20−22,28,37,41] In order to study the configuration of INA molecules adsorbed onto gold, SERS measurements under different conditions were performed. The roughened gold substrates were immersed in acidic or alkaline INA solutions for 36 h and then rinsed with base solution of the same pH to avoid any effect of proton concentration.

Figure 2 shows the SERS spectra obtained for INA SAMS prepared by dipping in acidic (Figure 2c) and alkaline (Figure 2e) INA solutions. In addition, Raman spectra of solid INA (Figure 2a) and INA aqueous solutions with the same pH values (Figure 2b,d) are included for comparison. When comparing the SERS and Raman spectra for equal pH conditions, for those vibrational modes that are directly involved in the INA−Au interaction a shifting of about 5−20 cm^{-1} as well as changes in their relative intensities are seen. For INA SAMS under both pH conditions, "in-plane" ring vibration modes are present (Figure 2c,e):[20,21,37] 1008−1019 cm^{-1} δCH (1), 1646−1606 cm^{-1} νCC(8a), and 1207−1211 cm^{-1} νCH(9a). Additionally, comparing with solid Raman spectrum (Figure 2a), the "out -of-plane" modes τCCCC(4) at 462 cm^{-1} and τCCCC(10a) at 778 cm^{-1} are absent, indicating that INA

DOI: 10.1021/acs.jpcc.5b11146
J. Phys. Chem. C 2016, 120, 4364−4372

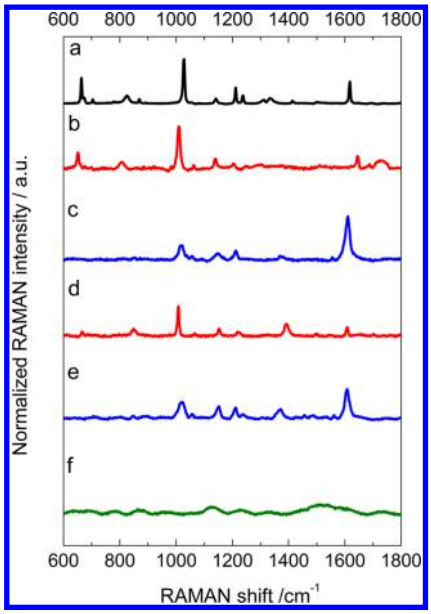

Figure 2. Raman spectra for solid INA (a), 0.1 M INA pH 0.3 (b), and 0.1 M INA pH 13 (d) aqueous solutions; SERS spectra for SAMs of INA on Au prepared by 36 h dipping in acid (c) and alkaline (e) solutions. (f) The same surface as in (e) after subsequent immersion for 10 min in a 1 M H_2SO_4, pH 0.3, solution.

molecules would adopt a perpendicular or slightly tilted alignment to the gold surface. On the other hand, for both dipping conditions, an enhancement of the νOCO^- at 1372 cm^{-1} and the absence of $\nu C{=}O$ at 1726 cm^{-1} are clearly seen. These results show that even for $pH_{dipping} < pK_{a,1}$, the INA molecules interact with gold atoms via the deprotonated carboxylic group. Similar behavior has been described previously for INA adsorbed on Ag[20,21,37] or 2-mercaptonicotinic acid on Au(111).[8]

In order to obtain additional information on the stability of INA SAMS with changes in pH, a SERS experiment in conditions similar to those described above for the electrochemical results (Figure 1) was performed. The modified gold surface by 36 h of dipping in 10 mM INA (pH 13) (Figure 2e) was subsequently immersed in a 1 M H_2SO_4 (pH 0.3) solution for 10 min, and after that a new SERS spectrum was recorded (Figure 2f). As for the electrochemical results, the spectrum shows a complete loss of INA Raman signals, indicating that INA molecules were removed from the gold surface after the immersion in an environment where $pH < pK_{a,1}$.

In summary, electrochemical results allow concluding that SAMS of INA are formed by immersion of the gold substrates in INA aqueous solutions of different pH. Inhibition of the electrochemical activity of the Fe^{2+}/Fe^{3+} redox probe suggests that INA SAMS block the gold surface for the charge transfer reaction. Furthermore, in spite of the adsorption is made in acidic ($pH < pK_{a,1}$) or alkaline conditions ($pH > pK_{a,2}$), INA molecules interact perpendicularly with the gold surface through the deprotonated carboxylic group. This behavior is associated with the displacement of the acid−base equilibrium, where a more favorable energetic interaction of the adsorbate with the metallic substrate and lateral interactions between neighbor molecules take place. Also, due to the acidic condition needed for the Fe^{2+}/Fe^{3+} redox couple performance, the voltammetric results allow obtaining information concerning the stability of the INA SAMS with respect to pH modifications, which was corroborated by SERS measurements. Because of the carboxylate group interacts directly with the gold surface, for SAMS prepared in alkaline media a high proton concentration enables the protonation of the carboxylate group and then destabilizes the monolayer. Contrarily, when the monolayer is generated in acidic solution, protons may have an important role in the SAM stabilization via hydrogen bonds between protonated pyridine rings of INA neighbor molecules.

Theoretical Results. *Adsorption Characterization.* In the previous section, we showed that INA molecules are adsorbed perpendicularly on the Au(111) surface via the carboxylate group. In order to explain these results and obtain more insight into the INA adsorption mechanism, DFT calculations for the different hypothetical interactions between INA molecules and the gold substrate were performed. For every case the adsorption energy, E_{ads}, is calculated according to

$$E_{ads} = E_{A/Au(111)} - E_A - E_{Au(111)} \quad (1)$$

where $E_{A/Au(111)}$ is the energy of the adsorbed species (anion or neutral molecule) and E_A and $E_{Au(111)}$ are the energies of the adsorbate and the surface, respectively. In the case of the anion species, we consider the INA dissociation state as the reference in order to obtain an adequate representation of the adsorption of charged species.

Also, the total charge is calculated as

$$Q_{total} = \sum qi \quad (2)$$

where Q_{total} is the sum of the Mulliken atomic charge q_i over all atoms in the given species. The INA layers have C_{3v} symmetry

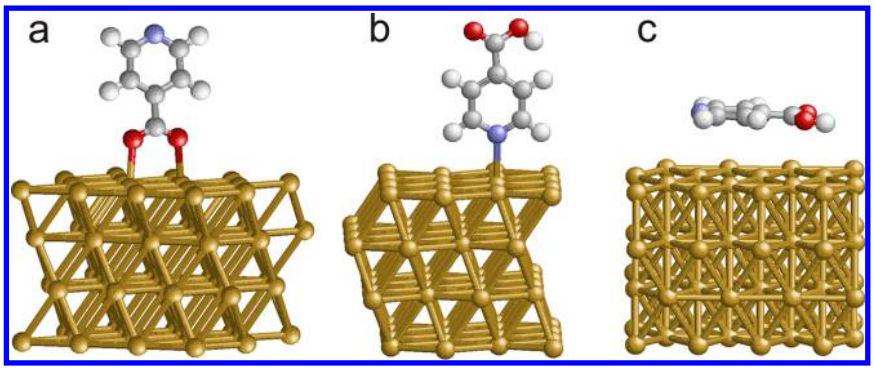

Figure 3. Schematic representation for different configurations of INA adsorbed on Au(111): anionic INA bonded through carboxylate group on bridge surface site (a); INA molecule bonded on top through the nitrogen atom of the pyridine ring (b) and parallel to the surface (c).

DOI: 10.1021/acs.jpcc.5b11146
J. Phys. Chem. C 2016, 120, 4364−4372

and were studied for the coverage values 0.0625, 0.143, 0.25, and 0.33, corresponding to $p(4 \times 4)$, $(\sqrt{7} \times \sqrt{7})R19.1°$, $p(2 \times 2)$, and $(\sqrt{3} \times \sqrt{3})R30°$ adlayers structures, respectively. Furthermore, for the determination of the preferential adsorption site we consider the lowest coverage, $\Theta = 0.0625$, which corresponds to a $p(4 \times 4)$ structure, taking into account the boundary conditions. According to Kučera and Gross,[42] at distances higher than 3 times the nearest-neighbors distance, the interaction between adsorbate molecules is negligible (i.e., a $p(3 \times 3)$ structure).

Figure 3 shows schematically some of the different INA adsorption geometries explored, namely anionic INA bonded through the carboxylate group on bridge surface sites (Figure 3a), neutral INA molecule bonded through the nitrogen atom of the pyridine ring on top sites (Figure 3b), or INA molecule adsorbed parallel to the Au(111) surface (Figure 3c). Additionally, Table 1 lists the adsorption energy and total charge calculated in atomic units (au) for selected species and configurations studied.

Table 1. Adsorption Energies and Mulliken Charges for Different Adsorption Configurations

INA species[a]	interacting group	substrate site	E_{ads} (eV)	Q_{total} (au)
	perpendicular configuration			
2′	−COOH	top	−0.47	0.09
	−*N*=	top	−0.81	0.03
3	$-COO^-$	bridge	−2.26	−0.39
	parallel configuration			
2′			−1.11	−0.02
3			−2.11	−0.46

[a]INA species denoted as shown in Scheme 1.

From the low adsorption energy values obtained for the neutral isonicotinic species (**2′**, see Scheme 1) in both parallel and perpendicular configurations, a weak INA−gold interaction is expected (physisorption type). Also, the negligible total charge calculated confirms the almost null interaction of neutral INA molecules to the gold surface. For this species (**2′**), the parallel configuration shows the strongest bond (E_{ads} = −1.11 eV) because of at this position both the carbonyl group and the N atom in the pyridine ring can simultaneously interact with the surface. Furthermore, for the perpendicular configuration a higher interaction through the nitrogen atom (E_{ads} = −0.81 eV) compared to that obtained for carboxyl group (−0.47 eV) is obtained.

On the other hand, the anionic species (**3**) shows higher adsorption energy (in absolute value) for both parallel and perpendicular configurations to the surface, indicating a stronger interaction with the gold atoms (chemical bond). Additionally, adsorption energy in bridge sites is energetically the most favorable (−2.26 eV). This value can be related to the fact that when anion species adsorbs on a bridge site, each oxygen atom interacts with one of two neighboring Au atoms (bidentate bond, Figure 3a). Also, the average total charge of ∼−0.4 au indicates that partial charge transference from the anion of INA to the Au surface takes place. These results indicate that the adsorption of the anionic species bonded to a bridge site in the Au(111) surface is the preferential configuration.

Table 2 lists the adsorption energies, the tilt angle β of the anions with respect to the normal vector, the distance between the oxygen and the surface ($d_{O-Au(111)}$), the Mulliken charge of INA molecules, and the Au surface charge for the anion species on bridge sites at the different coverage values studied. The tilt angle β is calculated as follows:

$$\cos(\beta) = \langle \nu_{C-N}, N \rangle / \| \nu_{C-N} \| \quad (3)$$

N and ν_{C-N} are the normal vector to the surface and the vector defined between the positions of the carboxyl C atom and the N atom in the pyridine ring, respectively. In addition, the surface charge can be calculated from the total charge eq 2 as

$$Q_{surface} = -Q_{total}/A \quad (4)$$

where $Q_{surface}$ is the surface charge and A is the substrate area per anion adsorbed.

As coverage increases, adsorption energy initially increases (from Θ values of 0.0625 to 0.143) and then decreases slightly (Table 2). Meanwhile, both the distance $d_{O-Au(111)}$ and the tilt angle (β) initially increase and then also show a slight decrease. Surface charge increases steadily (Table 2) due to the increase in the number of adsorbed species per unit area. This apparently complex dependence is attributed to the different interactions that take place as coverage changes. Taking into account the electrostatic repulsion between the anionic species of adsorbed INA alone, a continuous decrease in E_{ads} should be expected as coverage increases. For low coverage values (structures p(4 × 4) and $(\sqrt{7} \times \sqrt{7})R19.1°$), the initial increase in E_{ads} is attributed to the attractive $\pi-\pi$ interaction between aromatic rings. For higher coverage values (structures $p(2 \times 2)$ and $(\sqrt{3} \times \sqrt{3})R30°$) the electrostatic repulsive lateral interactions become more important than the attractive $\pi-\pi$ interaction between aromatic rings. As the surface coverage increases, the distance between the anionic species decreases (11.85, 7.84, 5.92, and 5.13 Å, respectively).[43]

Figure 4a shows the analysis of the partial density of states (PDOS) corresponding to the lowest and highest coverage values (0.0625 and 0.33, respectively) for an aromatic carbon atom belonging to the ring. This analysis provides important information about $\pi-\pi$ interaction between the INA anions. The higher electron densities are those of the 2*p* orbitals, and the most significant change obtained is the disappearance of a peak corresponding to the $2p_x$ orbital at −2 eV (Figure 4a) and the higher dispersion of the $2p_y$ orbital in the same region.

Table 2. Adsorption Energies, Tilt Angle β of the Anions with Respect to the Normal Vector, Distance between the Oxygen and the Surface ($d_{O-Au(111)}$), Mulliken Charge of INA Molecules, and the Au Surface Charge for the Anion Specie on Bridge Site for the Different Coverages Studied (Θ)

substrate structure	Θ	E_{ads} (eV)	β	$d_{O-Au(111)}$ (Å)	Mulliken charge (au)	surface charge (μC cm^{-2})
$p(4 \times 4)$	0.0625	−2.26	3° 29′	2.29	−0.39	5.14
$(\sqrt{7} \times \sqrt{7})R19.1°$	0.143	−2.55	6° 20′	2.30	−0.38	11.44
$p(2 \times 2)$	0.25	−2.18	3° 34′	2.28	−0.36	18.97
$(\sqrt{3} \times \sqrt{3})R30°$	0.33	−2.20	4° 23′	2.31	−0.35	24.56

DOI: 10.1021/acs.jpcc.5b11146
J. Phys. Chem. C 2016, 120, 4364−4372

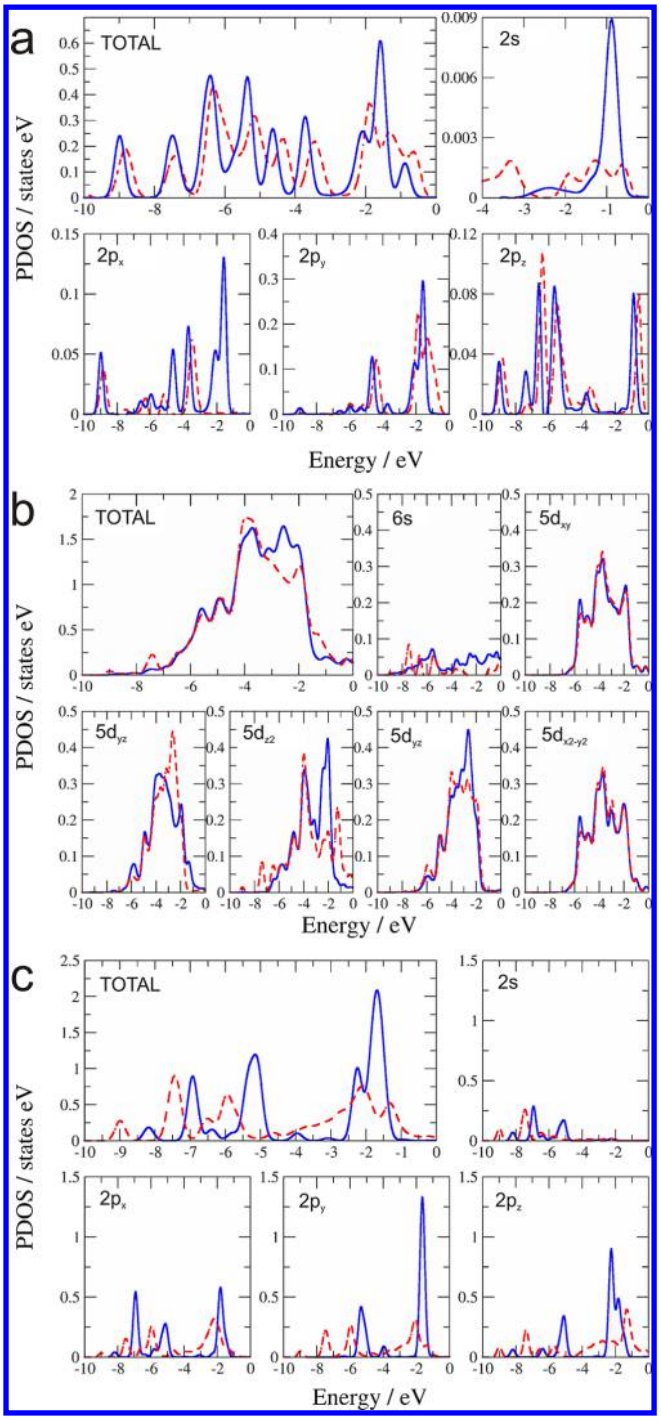

Figure 4. Total and individual PDOS corresponding to the valence orbitals for (a) an aromatic carbon atom belonging to the pyridinic ring at low and high coverage values Θ: 0.0625 (—) and 0.33 (- - -), (b) a gold atom involved in the bond to the INA anion on a bridge site at Θ = 0.0625 (- - -) and a free Au atom in a clean surface (—), and (c) one oxygen atom of adsorbed INA anion at Θ = 0.0625 (- - -) and a nonadsorbed INA anion in the vacuum (—). Zero energy corresponds to the Fermi level.

These changes are a clear evidence of a $\pi-\pi$ interaction between the aromatic rings. In conclusion, the effect of electrostatic repulsion and attractive $\pi-\pi$ interactions for high values of coverage are practically canceled, resulting in the changes in adsorption energy, distance $d_{O-Au(111)}$, and tilt angle shown in Table 2. In general, the tilt angle ranges from 3° to 6°, which is in agreement with spectroscopic evidence (see above) indicating that anionic INA species are adsorbed perpendicularly to the Au(111) surface. For all the studied adlayers, the anion−metal interaction is the most important, which gives commensurable ordered layers with the same symmetry of the substrate (C_{3v}).

Additionally, in the case of the adsorption through the N atom of the pyridine group to the Au surface, the bond distance for a top site is 2.42 Å. This value is higher than $d_{O-Au(111)}$ (see Table 2), which is in agreement with a weaker interaction through the nitrogen atom (physisorption).

INA−Au Interactions. In order to further analyze the chemical bond between the anionic isonicotinic acid adsorbed on a bridge site, the partial density of states (PDOS) for the gold atom involved in the bond to the INA anion was also calculated. This analysis gives valuable information about the atomic orbitals from the adsorbate (INA) and surface atoms (Au) that are involved in the chemical bond.[44] Figure 4b shows the energy dependence of the PDOS of a gold atom (on bridge sites at a coverage of 0.0625) compared to the PDOS of a free gold atom in a nonmodified surface. Because of $6s^1 5d^{10}$ electronic valence configuration is the most stable for Au atoms, the total PDOS as well as partial 6s and 5d atomic contributions are shown. Bonded Au atoms show modifications in the 6s, $5d_{yz}$, $5d_{xz}$, and $5d_{z^2}$ PDOS, while for $5d_{xy}$ and $5d_{x^2-y^2}$ orbitals the contributions remain unchanged. The calculated curves indicate that the main overlapping takes place involving the 5d atomic orbitals with z-axis symmetry while the 6s orbital has a lower contribution. On the other hand, the $x-y$ plane orbitals only participate in the bonds between the Au neighbor atoms in the metallic substrate.

In addition, Figure 4c shows the total and individual PDOS corresponding to the 2s and 2p valence orbitals for the oxygen atoms in the anion INA species adsorbed at a coverage of 0.0625 compared with the oxygen atom in the anion at the vacuum. For $2p_x$, $2p_y$, and $2p_z$, the modification observed in the PDOS contributions indicates that all the oxygen valence orbitals are involved in the bond with the z-symmetry 5d orbitals of the Au atom of the surface (see Figure 4b). In addition, a lower contribution of the 2s orbital of the oxygen is observed.

Adsorbate Mobility and SAMS Stability. Even though the molecules are adsorbed at the surface by a chemical bond, they can change in orientation in order to increase/decrease the coverage, move on terraces, jumping between neighboring sites, etc. In order to gain further insight in the adsorption characteristics of SAMS of INA on monocrystalline gold substrates, some calculations on common modification of the orientation and the diffusion of the adsorbate on the substrate surface were analyzed. The optimization of the minimum-energy path between the initial and final states was performed using the NEB method. The energy barrier allows estimating the jump frequency according to[44]

$$\upsilon = \upsilon_0 \exp[-E^{\#}/(k_B T)] \quad (5)$$

where υ_0, $E^{\#}$, k_B, and T are the frequency of attempts, the activation energy, the Boltzmann constant, and the absolute temperature (300 K), respectively. For the calculation, a typical value of pre-exponential factor υ_0 equal to 1×10^{13} s^{-1} was used.[35]

Figure 5 shows the minimum-energy path for the change in position from the parallel to the perpendicular configuration on a bridge site at low coverage. An activation energy of 0.12 eV,

DOI: 10.1021/acs.jpcc.5b11146
J. Phys. Chem. C 2016, 120, 4364−4372

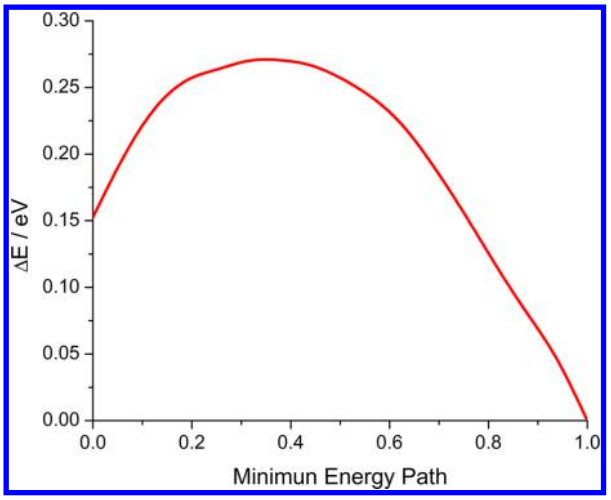

Figure 5. NEB energy path for the change of position of adsorbed INA anions on a bridge site from parallel to perpendicular configurations.

with $\upsilon_{\parallel\rightarrow\perp} = 9.64 \times 10^{10}$ s^{-1}, is estimated. From the energy profile (Figure 5), it is easy to see that the final perpendicular configuration is the more stable state. On the other way, the energy barrier for the opposite path is higher (0.27 eV, with $\upsilon_{\perp\rightarrow\parallel} = 2.91 \times 10^{8}$ s^{-1}), indicating that this process results kinetic and thermodynamically not favorable. In addition, the frequency ratio $\upsilon_{\parallel\rightarrow\perp}/\upsilon_{\perp\rightarrow\parallel}$ is a measurement of the amount of INA anions that change from a parallel to a perpendicular position. The estimated value of $\upsilon_{\parallel\rightarrow\perp}/\upsilon_{\perp\rightarrow\parallel} = 3.3 \times 10^{2}$ indicates that if an INA anion adsorbs parallel to the gold surface, exists a high probability that it may change its orientation to a perpendicular configuration.

On the other hand, it is also important to know the mobility of the anion on the surface because (i) it might prevent an electrochemical probe approaching to the surface and (ii) the surface diffusion on the terraces favors the aggregate or islands nucleation, growth, and ripening processes. Then, the analysis of energies involved in the surface diffusion of an INA anion bonded via the carboxylate group between two neighboring bridge sites was performed. The projection of the minimum energy path (MEP) onto the Au(111) surface is shown in Figure 6a. In the case of the C atom from the carboxylate group, the path is linear from the starting to the end point, passing near to a gold top site corresponding to the third gold layer in the slab (hcp site) and then near to a top site from the second gold layer (fcc site) until arriving to the neighboring bridge site. The O atoms of the carboxylate group interact directly with the surface suffering greater geometry changes, which is related to the energy changes. The energy profile (MEP) obtained from the initial to the final position, presents one maximum with a shoulder (Figure 6b). The maximum (‡1) corresponds to the crossing on the hcp site and the shoulder (‡2) through the fcc site. The higher energy barrier (‡1) is ca. 0.27 eV and, according to eq 5, a hopping frequency of 2.91×10^{8} s^{-1} at 300 K can be calculated. Additionally, from this frequency, a surface diffusion coefficient can be estimated as[45]

$$D = \upsilon d^2/z \tag{6}$$

where d is the distance between two neighboring bridge sites (2.96 Å) and z is the number of nearest sites ($z = 4$). Therefore, a surface diffusion coefficient $D = 4.80 \times 10^{-8}$ cm^2 s^{-1} is estimated. The diffusion of a molecule on a surface is a complex process, which depends on the torsional configuration

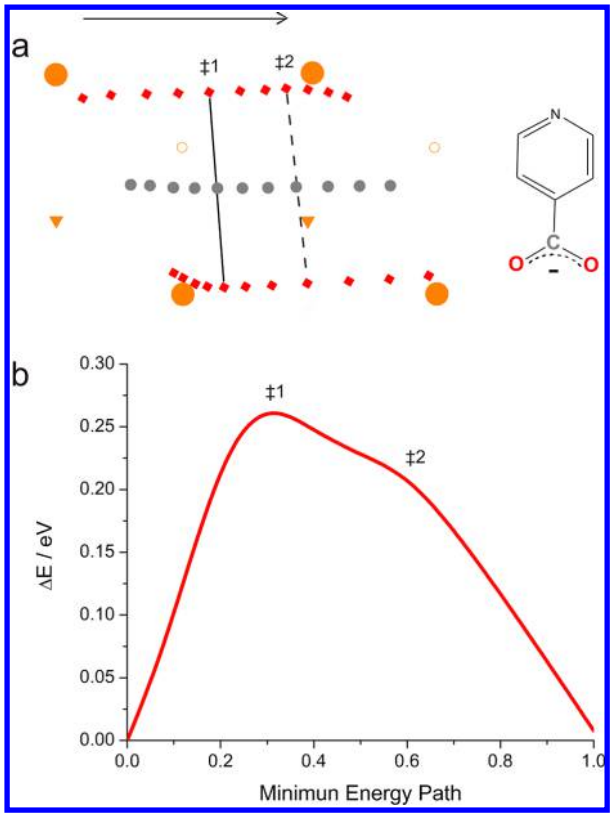

Figure 6. NEB energy path for the diffusion of an adsorbed INA anion between two equivalent bridge sites. (a) Projection and (b) energy profile (MEP). (●) Gold surface atoms; (▼) gold atoms from the second layer; (○) gold atoms from the third layer; (small gray circle) carbon atom of carboxylate group; (◆) oxygen atoms of the carboxylate group. For meaning of ‡1 and ‡2, see text.

of the adsorbate and the degrees of freedom. The present results show that the diffusion barrier is rather low, thus allowing the diffusion of the INA anions on the gold surface.

Another interesting point to analyze is the stability of the adsorbates when a dissolved species such as the hydronium ion comes close to the SAM. This interaction was studied by means of a simple geometry optimization using the conjugate gradient (CG) algorithm. Figure 7a shows the change in energy between the calculated energy for a new geometry with reference to the energy of the final configuration as a function of number of conjugated gradient steps.

For better understanding, four configurations are schematically shown in Figure 7b. The initial state (I) is a hydronium ion (solvated proton) close to the INA anion adsorbed on a gold bridge site. During the optimization, the hydronium ion interacts with the gold surface near to the carboxylate group of an INA anion (II). Then, a hydrogen atom of the hydronium ion interacts with one of oxygen atoms of carboxylate neighbor group, unbinding this oxygen from the surface (III). Finally, the complete protonation of the carboxylate group takes place, leading to the complete desorption of the INA molecule together with a water molecule (IV). The change in energy in the overall process (−2.4 eV) indicates a high stabilization of the system. Then, the experimental observation about the instability of the INA monolayers in strongly acidic media can be explained.

In summary, vdW-DFT results are in good agreement with experimental data shown, where the analysis of SERS spectra

DOI: 10.1021/acs.jpcc.5b11146
J. Phys. Chem. C 2016, 120, 4364−4372

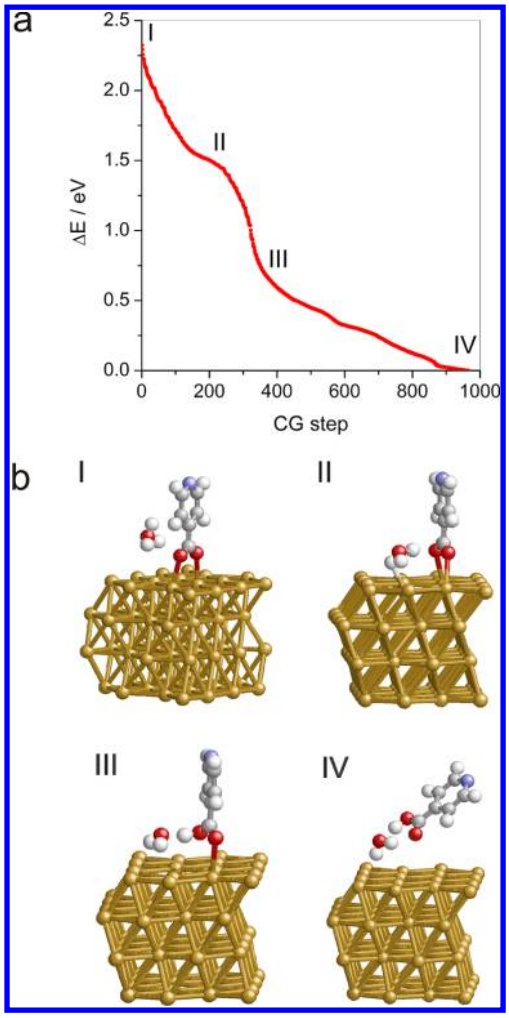

Figure 7. (a) Gradient conjugated energy change as a function of the number of conjugated gradient steps for the interaction of an adsorbed INA anion on a bridge site with a hydronium ion. (b) I to IV: schematic representation of selected configurations (see text).

indicates that the SAMS present the anionic INA species interacting mainly through the carboxylate group to the gold surface. Also, for all the values of coverage studied, the tilt angle is always small, indicating that INA anions are adsorbed perpendicularly to the Au surface or slightly tilted from the normal vector. Additionally, if INA molecules adsorb parallel to the surface, the change in orientation to a perpendicular configuration is a kinetic and thermodynamically favorable process at room temperature. Also, although INA is adsorbed to the surface by a chemical bond, the diffusion between neighboring bridge sites and the interaction with hydronium ions are surface processes energetically probable. Finally, PDOS analysis for the gold and oxygen atomic orbitals for bonded INA–Au indicates that the main interactions take place via the *z*-axis 5d gold orbitals and 2p oxygen atomic orbitals.

CONCLUSIONS

Self-assembled monolayers of isonicotinic acid on Au(111) were prepared by the immersion method in INA aqueous solutions at different pH values. The presence of SAMS on the surface is evidenced by the change in the kinetics of the electron transfer reaction for the Fe^{2+}/Fe^{3+} redox probe. For both acidic and alkaline dipping conditions, SERS spectra show the presence of the in-plane ring signals and the stretching of COO^- group along with the absence of the out-of-plane signals.

These results indicate that INA adsorbs on the gold surface through the deprotonated carboxylate group, either perpendicularly or slightly tilted with respect to the normal. In this configuration the layer leaves the pyridinic group in contact with the electrolyte, being sensitive to pH modifications.

The adsorption energies for different configurations of INA on Au(111) obtained from DFT calculations including van der Waals interactions at selected coverage values indicate that the preferential interactions correspond to the anionic species of INA that adsorbs to the gold surface in bridge sites, which correlates well with the experimental findings. In addition, due to the ionizable group involved in the molecular anchorage (deprotonated carboxylate group), some instability of the SAMS is experimentally observed by modification of the pH of the chemical environment.

At low coverage, the anion can be chemically bonded to the surface in parallel or perpendicular positions. Despite this, the low energy barrier for changing from parallel to perpendicular configurations indicates that the perpendicular configuration of the INA molecules is more stable, corroborating the SERS results. Also, although the INA anions are adsorbed to the surface through a chemical bond, the diffusion between neighboring bridge sites as well as the SAMS desorption due to the presence of hydronium ions are energetically possible surface process.

AUTHOR INFORMATION

Corresponding Authors

*Tel +54 351 5353866; fax +54 351 4334188; e-mail mlopez@fcq.unc.edu.ar (M.L.T.).

*Tel +54 351 5353866; fax +54 351 4334188; e-mail mrojas@fcq.unc.edu.ar (M.I.R.).

Notes

The authors declare no competing financial interest.

ACKNOWLEDGMENTS

This work was supported by PIP 11220120100031 and 11220090100720 from CONICET. SECyT UNC, CCAD-UNC, and GPGPU Computing group, Argentina, are also acknowledged. M. L. Para thanks CONICET for the doctoral fellowship. Raman facilities at "Laboratorio de Nanoscopía y Nanofotónica", INFIQC–CONICET/UNC, "Sistema Nacional de Microscopía", MINCyT, are gratefully acknowledged.

REFERENCES

(1) Calvo, E. J.; Rothacher, M. S.; Bonazzola, C.; Wheeldon, I. R.; Salvarezza, R. C.; Vela, M. E.; Benítez, G. Biomimetics with a Self-Assembled Monolayer of Catalytically Active Tethered Isoalloxazine on Au. *Langmuir* **2005**, *21*, 7907–7911.

(2) Urcuyo, R.; Cortés, E.; Rubert, A. A.; Benítez, G.; Montero, M. L.; Tognalli, N. G.; Fainstein, A.; Vela, M. E.; Salvarezza, R. C. Aromatic and Aliphatic Thiol Self-Assembled Monolayers on Au: Anchoring and Delivering Copper Species. *J. Phys. Chem. C* **2011**, *115*, 24707–24717.

(3) Nagahara, T.; Suemasu, T.; Aida, M.; Ishibashi, T. Self-Assambled Monolayers of Double-Chain Disulfides of Adenine on Au: An IR-UV Sum-Frequency Generation Spectroscopic Study. *Langmuir* **2010**, *26*, 389–396.

(4) Huang, Y.; Wu, D.; Wang, A.; Ren, B.; Rondinini, S.; Tian, Z.; Amatore, C. Bridging the Gap between Electrochemical and Organometallic Silver Cathodes. *J. Am. Chem. Soc.* **2010**, *132*, 17199–17210.

DOI: 10.1021/acs.jpcc.5b11146
J. Phys. Chem. C 2016, 120, 4364–4372

(5) Dou, R.; Ma, X.; Xi, L.; Yip, H. L.; Wong, K. Y.; Lau, W. M.; Jia, J.; Xue, Q.; Yang, W.; Ma, H.; Jen, A. K. Self-Assembled Monolayer of Aromatic Thiols Stabilized by Parallel-Displaced π-π Stacking Interactions. *Langmuir* **2006**, *22*, 3049−3056.
(6) Li, H.; Xu, B.; Evans, D.; Reutt-Robey, J. Isonicotinic Acid Molecular Films on Ag(111): I. XPS and STM Studies of Orientational Domains. *J. Phys. Chem. C* **2007**, *111*, 2102−2106.
(7) Barrena, E.; Ocal, C.; Salieron, M. Evolution of the structure and mechanical stability of self-assambed alkanothiol island on Au(111) due to diffusion and ripening. *J. Chem. Phys.* **1999**, *111*, 9797−9802.
(8) Pissinis, D. E.; Linarez Pérez, O. E.; Cometto, F. P.; López Teijelo, M. Preparation and characterization of self assembled monolayers of 2-mercaptonicotinic acid on Au(111). *J. Electroanal. Chem.* **2014**, *712*, 167−177.
(9) Euti, E. M.; Vélez Romero, P.; Linarez Pérez, O. E.; Ruano, G.; Patrito, E. M.; Zampieri, G.; Leiva, E. P. M.; Macagno, V. A.; Cometto, F. P. Electrochemical, HR-XPS and SERS study of the self-assembly of biphenyl 4,4′-dithiol on Au(111) from solution phase. *Surf. Sci.* **2014**, *630*, 101−108.
(10) Cometto, F. P.; Patrito, E. M.; Paredes Olivera, P.; Zampieri, G.; Ascolani, H. Electrochemical High-Resolution Photoemission Spectroscopy and vdW-DFT Study of the Thermal Stability of Benzenethiol and Benzeneselenol Monolayers on Au(111). *Langmuir* **2012**, *28*, 13624−13635.
(11) Pensa, E.; Rubert, A. A.; Benítez, G.; Carro, P.; González Orive, A.; Hernández Creus, A.; Salvarezza, R. C.; Vericat, C. Are 4-mercaptobenzoic acid self assembled monolayers on Au(111) a suitable system to test adatom models? *J. Phys. Chem. C* **2012**, *116*, 25765−25771.
(12) Paulo, T. de F.; Abruña, H. D.; Diógenes, I. C. N. Thermodynamic, kinetic, surface pKa, and structural aspects of self-assembled monolayers of thiol compounds on gold. *Langmuir* **2012**, *28*, 17825−17831.
(13) Wen, R.; Fang, Y. Adsorption of pyridine carboxylic acids on silver surface investigated by potential-dependent SERS. *Vib. Spectrosc.* **2005**, *39*, 106−113.
(14) Barthelmes, J.; Plieth, W. SERS investigations on the adsorption of pyridine carboxylic acids on silver − Influence of pH and supporting electrolyte. *Electrochim. Acta* **1995**, *40*, 2487−2490.
(15) Andreasen, G.; Vela, M. E.; Salvarezza, R. C.; Arvia, A. J. Influence of the electric potential on the structure of pyridine adlayers on Au(111) terraces from in-situ scanning tunnelling microscopy imaging. *J. Electroanal. Chem.* **1999**, *467*, 230−237.
(16) Iost, R. M.; Crespilho, F. N. Layer-by-layer self-assembly and electrochemistry: Applications in biosensing and bioelectronics. *Biosens. Bioelectron.* **2012**, *31*, 1−10.
(17) Benkstein, K. D.; Martinez, C. J.; Li, G.; Meier, D. C.; Montgomery, C. B.; Semancik, S. Integration of nanostructured materials with MEMS microhotplate platforms to enhance chemical sensor performance. *J. Nanopart. Res.* **2006**, *8*, 809−822.
(18) Chazalviel, J. N.; Allongue, P. On the origin of the efficient nanoparticle mediated electron transfer across a self-assembled monolayer. *J. Am. Chem. Soc.* **2011**, *133*, 762−764.
(19) Kissling, G.; Miles, D. O.; Fermín, D. J. Electrochemical charge transfer mediated by metal nanoparticles and quantum dots. *Phys. Chem. Chem. Phys.* **2011**, *13*, 21175−21185.
(20) Wen, R.; Fang, Y. Adsorption of pyridine carboxylic acids on silver surface investigated by potential-dependent SERS. *Vib. Spectrosc.* **2005**, *39*, 106−113.
(21) Park, S. M.; Kim, K.; Kim, M. S. Raman spectroscopy of isonicotinic acid adsorbed onto silver sol surface. *J. Mol. Struct.* **1994**, *328*, 169−178.
(22) Nogueira, H. I. S. Surface-enhanced Raman scattering (SERS) of 3-aminosalicylic and 2-mercaptonicotinic acids in silver colloids. *Spectrochim. Acta, Part A* **1998**, *54*, 1461−1470.
(23) Soler, J. M.; Artacho, E.; Gale, J. D.; García, A.; Junquera, J.; Ordejón, P.; Sánchez-Portal, D. The SIESTA method for ab initio order-N materials simulation. *J. Phys.: Condens. Matter* **2002**, *14*, 2745−2779.
(24) Grimme, S. Semiempirical GGA-Type Density Functional Constructed with a Long-Range Dispersion Correction. *J. Comput. Chem.* **2006**, *27*, 1787−1799.
(25) Tonigold, K.; Gross, A. Adsorption of small aromatic molecules on the (111) surfaces of noble metals: a DFT study with semi-empirical corrections for dispersion effects. *J. Chem. Phys.* **2010**, *132*, 224701−224701−10.
(26) Göltl, F.; Grüneis, A.; Bučko, T.; Hafner, J. Van der Waals interactions between hydrocarbon molecules and zeolites: Periodic calculations at different levels of theory, from density functional theory to the random phase approximation and Møller-Plesset perturbation theory. *J. Chem. Phys.* **2012**, *137*, 114111−114111−17.
(27) Wilson, E. B. The normal modes and frequencies of vibration of the regular plane hexagon model of the benzene molecule. *Phys. Rev.* **1934**, *45*, 706−714.
(28) Lord, R. C.; Marston, A. L.; Miller, F. A. Infra-red and Raman spectra of the diazines. *Spectrochim. Acta* **1957**, *9*, 113−125.
(29) Tognalli, N. G.; Fainstein, A.; Vericat, C.; Vela, M. E.; Salvarezza, R. C. Exploring three-dimensional nanosystems with Raman spectroscopy: methylene blue adsorbed on thiol and sulfur monolayers on gold. *J. Phys. Chem. B* **2006**, *110*, 354−360.
(30) Troullier, N.; Martins, J. L. Efficient pseudopotentials for plane-wave calculations. *Phys. Rev. B: Condens. Matter Mater. Phys.* **1991**, *43*, 1993−2006.
(31) Kleinman, L.; Bylander, D. M. Efficacious Form for Model Pseudopotentials. *Phys. Rev. Lett.* **1982**, *48*, 1425−1428.
(32) Perdew, J. P.; Burke, K.; Ernzerhof, M. Generalized Gradient Approximation Made Simple. *Phys. Rev. Lett.* **1996**, *77*, 3865−3868.
(33) Press, W. H.; Flannery, B. P.; Teukolsky, S. A.; Vetterling, W. T. *Numerical Recipes: The Art of Scientific Computing*; Cambridge University Press: Cambridge, UK, 1986.
(34) Henkelman, G.; Uberuaga, B. P.; Jonsson, H. A. climbing nudged elastic band method for finding saddle points and minimum energy paths. *J. Chem. Phys.* **2000**, *113*, 9901−9904.
(35) Henkelman, G.; Jonsson, H. Improved tangent estimate in the nudged elastic band method for finding minimum energy path and saddle points. *J. Chem. Phys.* **2000**, *113*, 9978−9985.
(36) Szabo, A.; Ostlung, N. S. *Modern Quantum Chemistry*; McGraw-Hill: New York, 1989; pp 149−152, 203 ff.
(37) Barthelmes, J.; Plieth, W. SERS Investigations on the adsorption of pyridine carboxylic acids on silver: influence of pH and supporting electrolyte. *Electrochim. Acta* **1995**, *40*, 2487−249.
(38) Amatore, C.; Savéant, J. M.; Tessier, D. Charge transfer at partially blocked surfaces. A model for the case of microscopic active and inactive sites. *J. Electroanal. Chem. Interfacial Electrochem.* **1983**, *147*, 39−51.
(39) Finklea, H. O.; Snider, D. A.; Fedik, J.; Sabatani, E.; Gafni, Y.; Rubinstein, I. Characterization of octadecanethiol-coated gold electrodes as microarray electrodes by cyclic voltammetry and ac impedance spectroscopy. *Langmuir* **1993**, *9*, 3660−3667.
(40) Nicholson, R. S.; Shain, I. Theory of stationary electrode polarography. Single Scan and cyclic methods applied to reversible, irreversible, and kinetic Systems. *Anal. Chem.* **1964**, *36*, 706−723.
(41) Gao, J.; Hu, Y.; Li, S.; Zhang, Y.; Chen, X. Adsorption of benzoic acid, phthalic acid on gold substrates studied by surface-enhanced Raman spectroscopy and density functional calculations. *Spectrochim. Acta, Part A* **2013**, *104*, 41−47.
(42) Kučera, J.; Gross, A. Adsorption of 4-Mercaptopyrine on Au(111): A Periodic DFT Study. *Langmuir* **2008**, *24*, 13985−13992.
(43) Sinnokrot, M. O.; Valeev, E. F.; Sherrill, C. D. Estimates of the Ab Initio Limit for π−π Interactions: The Benzene Dimer. *J. Am. Chem. Soc.* **2002**, *124*, 10887−10893.
(44) Martin, R. M. Periodic solids and electron bands. In *Electronic Structure: Basic Theory and Practical Methods*; Cambridge University Press: Cambridge, UK, 2004; pp 73−96.
(45) Hill, T. L. *An Introduction to Statistical Thermodynamics*; Addison-Wesley Publishing Co.: Boston, MA, 1960.

DOI: 10.1021/acs.jpcc.5b11146
J. Phys. Chem. C 2016, 120, 4364−4372